

Selecting factor of safety against liquefaction for design based on cost considerations

S. Upadhyaya, R.A. Green & A. Rodriguez-Marek

Department of Civil and Environmental Engineering, Virginia Tech, USA

B.W. Maurer

Department of Civil and Environmental Engineering, University of Washington, USA

ABSTRACT: The stress-based simplified procedure is the most widely used approach for evaluating liquefaction triggering-potential of sandy soils. In deterministic liquefaction evaluations, “rules of thumb” are typically used to select the minimum acceptable factor of safety (FS) against liquefaction triggering, sometimes guided by the strain potential of the soil once liquefied. This approach does not fully consider the value of the infrastructure that will potentially be impacted by the liquefaction response of the soil. Accordingly, in lieu of selecting FS based solely on precedent, Receiver Operator Characteristic (ROC) analyses are used herein to analyze the Standard Penetration Test (SPT) liquefaction case-history database of Boulanger & Idriss (2014) to relate FS to the relative consequences of misprediction. These consequences can be expressed as a ratio of the cost of a false-positive prediction to the cost of a false-negative prediction, such that decreasing cost-ratios indicate greater consequences of liquefaction, all else being equal. It is shown that FS = 1 determined using the Boulanger & Idriss (2014) procedure inherently corresponds to a cost ratio of ~0.1 for loose soils and ~0.7 for denser soils. Moreover, the relationship between FS and cost ratio provides a simple and rational approach by which the project-specific consequences of misprediction can be used to select an appropriate FS for decision making.

1 INTRODUCTION

The most commonly used approach for liquefaction-triggering evaluations is the stress-based simplified procedure originally developed by Whitman (1971) and Seed & Idriss (1971). Although probabilistic variants of this procedure have been developed, deterministic evaluations still represent the standard of practice. In a deterministic liquefaction evaluation procedure, the normalized cyclic stress ratio (CSR*), or seismic demand, and the normalized cyclic resistance ratio ($CRR_{M7.5}$), or soil capacity, are used to compute a factor of safety (FS) against liquefaction:

$$FS = \frac{CRR_{M7.5}}{CSR^*} \quad (1)$$

where CSR* is the cyclic stress ratio normalized to a M7.5 event and corrected to an effective overburden stress of 1 atm and level-ground conditions. $CRR_{M7.5}$ is the cyclic resistance ratio normalized to the same conditions as CSR* and is computed using semi-empirical relationships that are a function of in-situ test metrics, which have been normalized to overburden pressure and corrected for fines-content (e.g., Whitman 1971, Seed & Idriss 1971, Robertson & Wride 1998, Cetin et al. 2004, Moss et al. 2006, Idriss & Boulanger 2008, Kayen et al. 2013, Boulanger & Idriss 2014, among others). These normalized in-situ metrics include Standard

Penetration Test (SPT) blow count ($N_{160\text{cs}}$); Cone Penetration Test (CPT) tip resistance ($q_{c1\text{Ncs}}$); and shear-wave velocity (V_{s1}).

Liquefaction is predicted to trigger when $FS \leq 1$ (i.e., when the demand equals or exceeds the capacity). In current practice, “rules of thumb” are often used to select an appropriate FS for design. While such rules-of-thumb should, in theory, account for the consequences, or costs, of misprediction, they have generally been based largely on heuristic techniques and intuition. Due to the lack of a standardized approach to selecting FS, various guidelines have been proposed, often without any consideration of misprediction consequences. These include the costs of false-negative predictions (i.e., liquefaction is observed, but is not predicted), which are the costs of liquefaction-induced damage; and the costs of false-positive predictions (i.e., liquefaction is predicted, but not is not observed), which could be those associated with ground improvement. Clearly, these costs can vary among different engineering projects. For example, the costs associated with mispredicting liquefaction beneath a one-story residential building will be likely very different than those from a similar misprediction beneath a large earthen dam.

Accordingly, the focus of the study presented herein is to investigate the relationship between the costs of misprediction and appropriate FS values using a standardized, quantitative approach. Towards this end, Receiver Operating Characteristic (ROC) analyses are used to analyze the SPT case-history database compiled by Boulanger & Idriss (2014) [BI14] to relate the FS computed using their SPT-based liquefaction triggering procedure to the ratio of false-positive costs to false-negative costs. This ratio is henceforth referred to as the cost ratio (CR). The resulting relationships between CR and FS provide insights into previously proposed FS guidelines and can be used to develop optimal, project-specific FS values for decision making.

2 DATA AND METHODOLOGY

This study utilizes the SPT-based case-history database compiled by BI14, which is comprised of 136 “liquefaction” cases (including 3 “marginal” cases) and 116 “no liquefaction” cases. Figure 1 shows the BI14 deterministic $CRR_{M7.5}$ curve along with the associated case history data. Histograms of the FS of the case histories are shown in Figure 2, where the case histories are divided into three groups: $N_{1,60\text{cs}} \leq 15$ blows/30 cm, $15 \text{ blows/30 cm} < N_{1,60\text{cs}} < 30$ blows/30 cm, and $N_{1,60\text{cs}} \geq 30$ blows/30 cm. The reason for this grouping will become apparent subsequently.

To investigate the relationship between FS and the costs of mispredicting liquefaction triggering, ROC analyses were performed on the FS distributions shown in Figure 2. A brief overview of ROC analysis is presented in the following section.

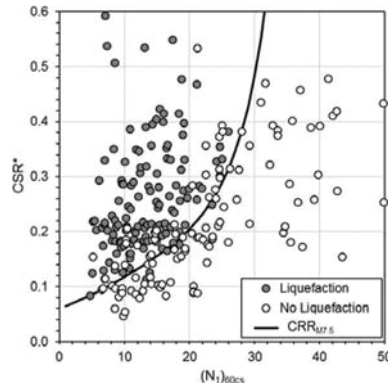


Figure 1. BI14 deterministic $CRR_{M7.5}$ curve and associated case history data.

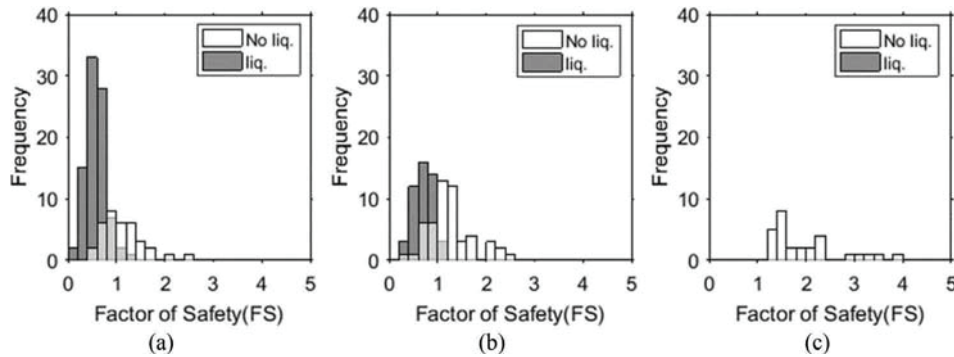


Figure 2. Histograms of FS for the BI14 SPT case history database: (a) $N_{1,60\text{cs}} \leq 15$ blows/30 cm; (b) $15 \text{ blows/30 cm} < N_{1,60\text{cs}} < 30 \text{ blows/30 cm}$; and (c) $N_{1,60\text{cs}} \geq 30 \text{ blows/30 cm}$. The light grey bars indicate the overlapping of the histograms of liquefaction and no liquefaction case histories.

2.1 Overview of ROC analyses

Receiver Operating Characteristics (ROC) analyses have been widely adopted to evaluate the performance of diagnostic models, including extensive use in medical diagnostics (e.g., Zou 2007) and to a much lesser degree in geotechnical engineering (e.g., Oommen et al. 2010, Maurer et al. 2015a,b,c, 2017a, b, c, Green et al. 2015, 2017, Zhu et al. 2017, Upadhyaya et al. 2018). In particular in cases where the distribution of “positives” (e.g., liquefaction cases) and “negatives” (e.g., no liquefaction cases) overlap (e.g., Figure 2a,b), ROC analyses can be used (1) to identify the optimum diagnostic threshold; and (2) to assess the relative efficacy of competing diagnostic models, independent of the thresholds used. A ROC curve is a plot of the True Positive Rate (R_{TP}) (i.e., liquefaction is predicted and was observed) versus the False Positive Rate (R_{FP}) (i.e., liquefaction is predicted, but was not observed) for varying threshold values (e.g., FS). A conceptual illustration of ROC analysis, including the relationship among the distributions for positives and negatives, the threshold value, and the ROC curve, is shown in Figure 3.

In ROC curve space, a diagnostic test that has no predictive ability (i.e., a random guess) will result in a ROC curve that plots as a 1:1 line through the origin. In contrast, a diagnostic test that has perfect predictive ability will result in a ROC curve that plots along the left

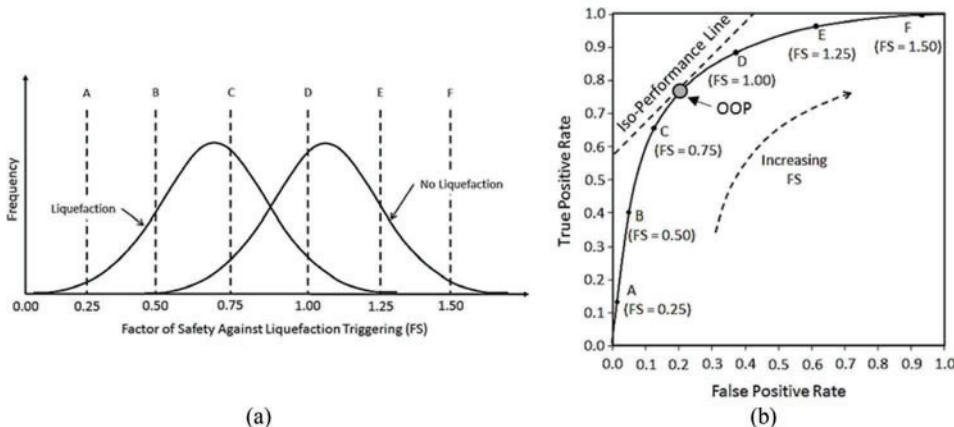


Figure 3. Conceptual illustration of ROC analyses: (a) frequency distributions of liquefaction and no liquefaction observations as a function of FS; (b) corresponding ROC curve.

vertical and upper horizontal axes, connecting at the point (0,1). This latter case indicates the existence of a threshold value that perfectly segregates the dataset (e.g., all cases with liquefaction have $FS \leq 1$ and all cases without liquefaction have $FS > 1$). The area under the ROC curve (AUC) can be used as a metric to evaluate the predictive performance of a diagnostic model, whereby higher AUC indicates better predictive capabilities (Fawcett 2005). As such, a random guess returns an AUC of 0.5 whereas a perfect model returns an AUC of 1.

The optimum operating point (OOP) in a ROC analysis is defined as the threshold value (e.g., FS) that minimizes the misprediction cost, where cost is computed as:

$$Cost = C_{FP} \times R_{FP} + C_{FN} \times R_{FN} \quad (2)$$

where C_{FP} and R_{FP} are the cost and rate of false-positive predictions, respectively, and C_{FN} and R_{FN} are the cost and rate of false-negative predictions, respectively. Normalizing Eq. (2) with respect to C_{FN} , and equating R_{FN} to $1 - R_{TP}$, cost may alternatively be expressed as:

$$Cost_n = Cost / C_{FN} = CR \times R_{FP} + (1 - R_{TP}) \quad (3)$$

where CR is the cost ratio defined by $CR = C_{FP}/C_{FN}$ (i.e., the ratio of the cost of a false-positive prediction to the cost of a false-negative prediction).

As may be surmised, Eq. 3 plots in ROC space as a straight line with slope of CR and can be thought of as a contour of equal performance (i.e., an iso-performance line). Thus, each CR corresponds to a different iso-performance line. One such line, with $CR = 1$ (i.e., false positives costs are equal to false-negative costs) is shown in Figure 3b. The point where the iso-performance line is tangent to the ROC curve corresponds to the OOP (e.g., the “optimal” FS corresponding to a given CR). Thus, by varying the CR values, a relationship between optimal FS and CR can be developed.

3 RESULTS AND DISCUSSION

ROC analyses were performed on the case history distributions shown in Figure 2a,b (note that a ROC analysis could not be performed on the distribution shown in Figure 2c because there are not any liquefaction case histories where $N_{1,60cs} \geq 30$ blows/30 cm). The resulting ROC curves are shown in Figure 4a. Using Eq. 3 in conjunction with these curves,

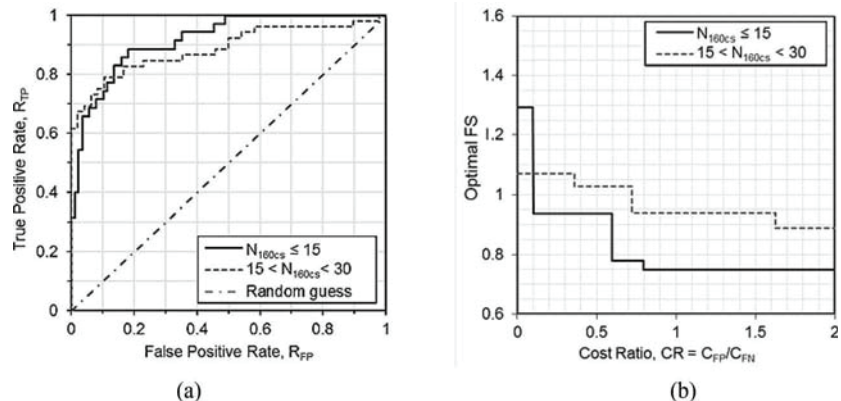


Figure 4. ROC analyses of the BI14 SPT case history data shown in Figure 2a ($N_{1,60cs} \leq 15$ blows/30 cm) and Figure 2b (15 blows/30 cm $< N_{1,60cs} < 30$ blows/30 cm): (a) ROC curves; and (b) optimal FS vs CR.

Table 1. Optimal FS for a range of CR

| CR | Optimal FS | |
|-----------|----------------------|------------------------|
| | $N_{1,60cs} \leq 15$ | $15 < N_{1,60cs} < 30$ |
| 0.00-0.10 | 1.29 | 1.07 |
| 0.10-0.36 | 0.94 | 1.07 |
| 0.36-0.60 | 0.94 | 1.03 |
| 0.60-0.72 | 0.78 | 1.03 |
| 0.72-0.80 | 0.78 | 0.94 |
| 0.80-1.63 | 0.75 | 0.94 |
| 1.63-2.00 | 0.75 | 0.89 |

relationships between CR and optimal FS were developed and are shown in Figure 4b. Moreover, the optimal FS for a range of CR are listed in Table 1.

As may be observed from Figure 4b, the optimal FS is inversely proportional to the CR (i.e., the lower the CR, the higher the degree of conservatism required). Additionally, it can be observed that the BI14 deterministic $CRR_{M7.5}$ curve (i.e., $FS = 1$) shown in Figure 1 has an associated CR of ~ 0.1 for $N_{1,60cs} \leq 15$ blows/30 cm and ~ 0.71 for $15 \text{ blows/30 cm} < N_{1,60cs} < 30 \text{ blows/30 cm}$. This implies a more conservative positioning of the $CRR_{M7.5}$ curve for looser soils than for denser soils. Whether this was intentional or not, this can be justified because of the higher strain potential of loose soils versus dense soils once liquefaction is triggered. In a similar vein, Martin & Lew (1999) propose FS guidelines for California considering different damage-potential modes of liquefaction (i.e., “settlement,” “surface manifestation,” and “lateral spreading”) where larger minimum required FS values are recommended for soils having $N_{1,60cs} \leq 15$ blows/30 cm versus soils having $N_{1,60cs} \geq 30$ blows/30 cm (Table 2).

As an example, if we evaluate the recommended minimum required FS for post-liquefaction consolidation settlement listed in Table 2 using Figure 4b, the $FS = 1.1$ for $N_{1,60cs} \leq 15$ blows/30 cm has an associated CR of ~ 0.1 (i.e., the cost associated with a false-positive prediction is about one tenth the cost of a false-negative prediction). If we assume that the FS varies linearly from 1.1 to 1.0 for $N_{1,60cs}$ ranging from 15 to 30 blows/30 cm, the associated CR ranges from 0 to ~ 0.71 . Again, the higher upper limit of the CR for denser soils can be justified based on the lower strain potential of the soil once it liquefies.

Although consideration of the strain potential of the liquefied soil should be taken into account in determining the minimum required FS for a project, the value of the infrastructure that will potentially be impacted by the liquefaction should also be considered (e.g., large earthen dam vs. a low-rise storage structure). This is where optimal FS-CR relationships shown in Figure 4b can be used to select project-specific FS. Specifically, the costs of liquefaction risk mitigation schemes relative to the costs associated with allowing the infrastructure to sustain damage (e.g., Green et al. 2019) can be taken directly into account in selecting the FS. This is conceptually illustrated in Figure 5 using a hypothetical optimal FS-CR curve. In this figure, the initial FS for a site is computed to be 1.0, which has an associated CR = 0.8.

Table 2. Minimum required FS for liquefaction hazard assessment for California (Martin & Lew 1999)

| Consequences of Liquefaction | $N_{1,60cs}$ | FS |
|------------------------------|--------------|-----|
| Settlement | ≤ 15 | 1.1 |
| | ≥ 30 | 1.0 |
| Surface Manifestation | ≤ 15 | 1.2 |
| | ≥ 30 | 1.0 |
| Lateral Spreading | ≤ 15 | 1.3 |
| | ≥ 30 | 1.0 |

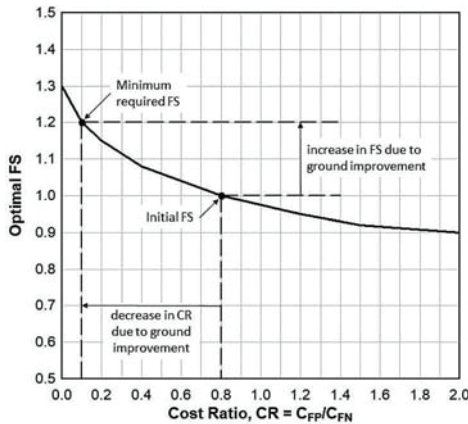


Figure 5. Conceptual illustration, using a hypothetical optimal FS-CR curve, on how to determine whether performing ground improvement to increase the FS from 1.0 to 1.2 is worth the expense.

However, the minimum required FS for the site is specified as 1.2, which has an associated $CR = 0.1$. To determine whether performing ground improvement to increase the FS from 1.0 to 1.2 is worth the expense, the difference between the CR for the unimproved and improved ground can be compared to the cost of ground improvement divided by C_{FN} (i.e., $CR_{improved} - CR_{unimproved}$ vs. Cost of Ground Improvement/ C_{FN}). If $(CR_{improved} - CR_{unimproved}) \geq \text{Cost of Ground Improvement}/C_{FN}$, then ground improvement is worth the expense (i.e., using a minimum required FS = 1.2 is justified). However, if $(CR_{improved} - CR_{unimproved}) < \text{Cost of Ground Improvement}/C_{FN}$, then it would be more economical to leave the site unimproved (i.e., use a minimum required FS = 1.0) and pay for the cost of repairs associated with liquefaction, if it occurs.

The limitation of using the optimal FS-CR curves in Figure 4b to select project-specific minimum required FS are the limited ranges of the FS represented by the curves (i.e., $N_{1,60cs} \leq 15$ blows/30 cm: $0.7 \leq FS \leq 1.3$; $15 \text{ blows}/30 \text{ cm} < N_{1,60cs} < 30 \text{ blows}/30 \text{ cm}$: $0.89 \leq FS \leq 1.075$). More specifically, the issue is the maximum value of the FS that can be determined using the curves (i.e., $FS = 1.3$ for $N_{1,60cs} \leq 15$ blows/30 cm and $FS \approx 1.075$ for $15 \text{ blows}/30 \text{ cm} < N_{1,60cs} < 30 \text{ blows}/30 \text{ cm}$), because it is doubtful that an FS less than 1.0 will be used as a design criterion. These upper bound limits on FS are dictated by the largest FS for the “liquefaction” case histories in distributions shown in Figure 2. And, although the distributions may become “smoother” as additional case histories are compiled, it is doubtful that the maximum FS represented by the optimal FS-CR curves will increase significantly. The reason is that the deterministic $CRR_{M7.5}$ curves are conservatively “placed” so that none of the “liquefaction” case histories have large FS; if they do, the deterministic $CRR_{M7.5}$ curve would be re-drawn to reduce the FS of the “liquefaction” case histories.

Inherently, selecting a minimum required FS for a project that is greater than 1.3 for $N_{1,60cs} \leq 15$ blows/30 cm or greater than 1.075 for $15 \text{ blows}/30 \text{ cm} < N_{1,60cs} < 30 \text{ blows}/30 \text{ cm}$ (e.g., $FS = 1.5$, Martin & Lew 1999) implies that the costs associated with allowing the infrastructure to sustain damage due to liquefaction are intolerable, regardless of the value of the impacted infrastructure. However, it needs to be realized that FS is based on both the capacity of the soil to resist liquefaction (i.e., $CRR_{M7.5}$) and the demand imposed on the soil due to earthquake shaking (i.e., CSR^*). For the case histories shown in Figure 1, best estimates of the ground motions actually experienced at the sites were used to compute CSR^* . However, for design specifications, ground motions having a given return period (T_R) are commonly used to compute CSR^* , where longer return period motions are specified for “critical” versus “standard” structures (e.g., ASCE 2005, 2017). Accordingly, the probability that liquefaction will be triggered at a site that is associated with common design specifications is a function of

both FS and the T_R of ground motions specified in design criteria, although this probability is not necessarily quantified. Based on this, the minimum required FS listed in Table 2, for example, could be used to form the basis of design specifications for both standard and critical facilities because the T_R of the design ground motions can be used to adjust the (unquantified) probability of liquefaction triggering to an acceptable level. Although this approach to specifying design criteria for liquefaction triggering may seem ad hoc, it does represent the current state-of-practice and will likely continue to do so until more formal probabilistic approaches for evaluating liquefaction triggering potential are developed (e.g., Green et al. 2018).

4 CONCLUSIONS

Utilizing the SPT liquefaction case-history database compiled by Boulanger & Idriss (2014), relationships between the optimal factor of safety against liquefaction (FS) and the ratio of false-positive prediction costs to false-negative prediction costs (i.e., cost ratio, CR) were developed. It was shown that an inverse relationship exists between CR and FS, such that as CR decreases, the corresponding optimal FS for decision making increases. The relationships were used to provide insights into FS specifications for California. The CR associated with minimum required FS for looser soils is lower than that for denser soils, due to the strain potential of the respective soils once liquefaction is triggered. However, these specifications do not consider the value of the infrastructure that will potentially be impacted by the liquefaction response of the soil; optimal FS-CR relationships can be used for this purpose. Specifically, optimal FS-CR relationships can be used to select the minimum required FS based on the costs of liquefaction risk-mitigation schemes relative to the costs associated with allowing the infrastructure to sustain damage.

ACKNOWLEDGEMENTS

This research was funded by National Science Foundation (NSF) grants CMMI-1435494, CMMI-1724575, CMMI-1751216, and CMMI-1825189, as well as Pacific Earthquake Engineering Research Center (PEER) grant 1132-NCTRBM and U.S. Geological Survey (USGS) award G18AP-00006. However, any opinions, findings, and conclusions or recommendations expressed in this paper are those of the authors and do not necessarily reflect the views of NSF, PEER, or USGS.

REFERENCES

American Society of Civil Engineering (ASCE), 2005. *ASCE/SEI 43-05: Seismic design criteria for structures, systems, and components in nuclear facilities*, American Society of Engineers, Reston, VA.

American Society of Civil Engineering (ASCE), 2017. *ASCE 7-16: Minimum design loads and associated criteria for buildings and other structures*, American Society of Engineers, Reston, VA.

Boulanger, R.W. & Idriss, I.M. 2014. *CPT and SPT based liquefaction triggering procedures*. Report No. UCD/CGM-14/01, Center for Geotechnical Modelling, Department of Civil and Environmental Engineering, UC Davis, CA, USA.

Cetin, K.O., Seed, R.B., Der Kiureghian, A., Tokimatsu, K., Harder, L.F., Jr., Kayen, R.E. & Moss, R. E.S. 2004. Standard penetration test-based probabilistic and deterministic assessment of seismic soil liquefaction potential. *Journal of Geotechnical and Geoenvironmental Engineering*, ASCE, 130(12): 1314–1340.

Fawcett, T. 2006. An introduction to ROC analysis. *Pattern recognition letters*, 27(8): 861–874.

Green, R.A., Maurer, B.W., Cubrinovski, M. & Bradley, B.A. 2015. Assessment of the Relative Predictive Capabilities of CPT-Based Liquefaction Evaluation Procedures: Lessons Learned from the 2010–2011 Canterbury Earthquake Sequence. *Proc. 6th Intern. Conf. on Earthquake Geotechnical Engineering* (6ICEGE), Christchurch, New Zealand, 2–4 November.

Green, R.A., Upadhyaya, S., Wood, C.M., Maurer, B.W., Cox, B.R., Wotherspoon, L., Bradley, B.A. & Cubrinovski M. 2017. Relative efficacy of CPT- versus Vs-based simplified liquefaction evaluation

procedures. *Proc. 19th Intern. Conf. on Soil Mechanics and Geotechnical Engineering*, Seoul, Korea, 17–22 September.

Green, R.A., Bommer, J.J., Rodriguez-Marek, A., Maurer, B., Stafford, P., Edwards, B., Kruiver, P.P., de Lange, G. & van Elk, J. 2018. Addressing limitations in existing ‘simplified’ liquefaction triggering evaluation procedures: Application to induced seismicity in the Groningen gas field,” *Bulletin of Earthquake Engineering*, <https://doi.org/10.1007/s10518-018-0489-3>.

Green, R.A., Wotherspoon, L.M. & Cubrinovski, M. 2019. Chapter 8: Damage and restoration to river stopbanks, *Earthquake-Flood Multi-Hazard Impacts on Lifeline Systems* (Sonia Giovinazzi, Deidre Hart, and Craig Davis, eds.), ASCE Monograph. (in press)

Idriss, I.M. & Boulanger, R.W. 2008. *Soil liquefaction during earthquakes*. Monograph MNO-12, Earthquake Engineering Research Institute, Oakland, CA, 261 pp.

Kayen, R., Moss, R., Thompson, E., Seed, R., Cetin, K., Kiureghian, A., Tanaka, Y. & Tokimatsu, K. 2013. Shear-wave velocity-based probabilistic and deterministic assessment of seismic soil liquefaction potential. *Journal of Geotechnical and Geoenvironmental Engineering*, 139(3): 407–419.

Martin, G.R. & Lew, M. (eds). 1999. *Recommended procedures for implementation of DMG Special Publication 117 guidelines for analysing and mitigating liquefaction in California*. Southern California Earthquake Center, University of Southern California, Los Angeles, CA.

Maurer, B.W., Green, R.A., Cubrinovski, M. & Bradley, B. 2015a. Fines-content effects on liquefaction hazard evaluation for infrastructure during the 2010–2011 Canterbury, New Zealand earthquake sequence. *Soil Dynamics and Earthquake Engineering*, 76: 58–68.

Maurer, B.W., Green, R.A., Cubrinovski, M., & Bradley, B. 2015b. Assessment of CPT-based methods for liquefaction evaluation in a liquefaction potential index framework. *Géotechnique* 65(5): 328–336.

Maurer, B.W., Green, R.A., Cubrinovski, M. & Bradley, B. 2015c. Calibrating the liquefaction severity number (LSN) for varying misprediction economies: A case study in Christchurch, New Zealand. *Proc. 6th International Conference on Earthquake Geotechnical Engineering*, Christchurch, New Zealand, 1–4 November 2015.

Maurer, B.W., Green, R.A., van Ballegooij, S., Bradley, B.A. & Upadhyaya, S. 2017a. Performance comparison of probabilistic and deterministic liquefaction triggering models for hazard assessment in 23 global earthquakes. *Geo-Risk 2017: Reliability-based design and code developments* (J. Huang, G.A. Fenton, L. Zhang, and D.V. Griffiths, eds.), ASCE Geotechnical Special Publication 283: 31–42.

Maurer, B.W., Green, R.A., van Ballegooij, S. & Wotherspoon, L. 2017b. Development of region-specific soil behavior type index correlations for evaluating liquefaction hazard in Christchurch, New Zealand. *Soil Dynamics and Earthquake Engineering*, (in press).

Maurer, B.W., Green, R.A., van Ballegooij, S. & Wotherspoon, L. 2017c. Assessing liquefaction susceptibility using the CPT Soil Behavior Type Index. *Proc. 3rd Intern. Conf. on Performance-Based Design in Earthquake Geotechnical Engineering (PBDIII)*, Vancouver, Canada, 16–19 July.

Moss, R.E.S., Seed, R.B., Kayen, R.E., Stewart, J.P., Der Kiureghian, A. & Cetin, K.O. 2006. CPT-based probabilistic and deterministic assessment of in situ seismic soil liquefaction potential. *Journal of Geotechnical and Geoenvironmental Engineering*, ASCE, 132(8):1032–1051.

Oommen, T., Baise, L.G. & Vogel, R. 2010. Validation and application of empirical liquefaction models. *Journal of Geotechnical and Geoenvironmental Engineering*, 136(12): 1618–1633.

Robertson, P.K. & Wride, C.E. 1998. Evaluating cyclic liquefaction potential using cone penetration test. *Canadian Geotechnical Journal*, 35(3): 442–459.

Seed, H.B. & Idriss, I.M. 1971. Simplified procedure for evaluating soil liquefaction potential. *Journal of the Soil Mechanics and Foundations Division*, 97(SM9): 1249–1273.

Upadhyaya, S., Maurer, B.W., Green, R.A., & Rodriguez-Marek, A. 2018. Effect of non-liquefiable high fines-content, high plasticity soils on liquefaction potential index (LPI) performance. *Geotechnical Earthquake Engineering and Soil Dynamics V: Liquefaction Triggering, Consequences, and Mitigation* (S.J. Brandenberg and M.T. Manzari, eds.), ASCE Geotechnical Special Publication 290: 191–198.

Whitman, R.V. 1971. Resistance of soil to liquefaction and settlement. *Soils and Foundations*, 11: 59–68.

Zhu, J., Baise, L.G. & Thompson, E.M. 2017. An updated geospatial liquefaction model for global application. *Bulletin of the Seismological Society of America*, 107(3), doi: 10.1785/0120160198.

Zou, K.H. 2007. Receiver operating characteristic (ROC) literature research. On-line bibliography available from: ",1,0,0><<http://www.spl.harvard.edu/archive/spl-pre2007/pages/ppl/zou/roc.html>> accessed 10 March 2016.